Molecular Design of Single-Site Metal Alkoxide Catalyst Precursors for Ring-Opening Polymerization Reactions Leading to Polyoxygenates. 1. Polylactide Formation by Achiral and Chiral Magnesium and Zinc Alkoxides, (η^3-L)MOR, Where L = Trispyrazolyl- and Trisindazolylborate Ligands

Malcolm H. Chisholm,* Nancy W. Eilerts, John C. Huffman, Suri S. Iyer, Martha Pacold, and Khamphee Phomphrai

Contribution from the Department of Chemistry, Indiana University, Bloomington, Indiana 47405

Received June 16, 2000

Abstract: Single-site achiral and chiral C_3-symmetric complexes LMOR, where M = Mg and Zn, L = an η^3-trispyrazolyl- or η^3-trisindazolyl-borate ligand and R = Et, ^{t}Bu, Ph, or $SiMe_3$, have been synthesized and employed in the ring-opening polymerization of L-, *rac*-, and *meso*-lactide in CH_2Cl_2 at 25 °C and below. The polymerization occurs by acyl cleavage and gives rise to polylactide, PLA, with PDI of 1.1−1.25 up to 90% conversion. Studies of the kinetics of polymerization reveal first order behavior in both lactide and metal catalyst. For L = tris(3-*tert*-butylpyrazolyl)borate, (^{t}Bupz)$_3$BH, polymerization of ∼500 equiv of L-lactide proceeds to 90% conversion within 1 h and 6 d for the magnesium and zinc catalysts, respectively. The zinc complexes are, however, more tolerant to air and moisture and solid samples where R = $SiMe_3$ are persistent in air for several days. The rate of polymerization is also significantly influenced by the nature of the η^3-L spectator ligand. Chiral C_3-symmetric catalysts, where L = tris(indazolyl)borates derived from camphor and menthone, show only slight enantioselectivity in their polymerization of *rac*-lactide but do show significant diastereoselectivity in their ability to preferentially polymerize *meso*-lactide from a mixture of *rac*- and *meso*-lactide. The poly(mesolactide) shows a modest preference for syndiotactic junctions, *RSRSRS*. The molecular structures, deduced from single-crystal X-ray crystallography, are reported for η^3-HB(3-Phpz)$_3$MgEt(THF), [η^3-HB((7*R*)-^{i}Pr-(4*R*)-Me-4,5,6,7-tetrahydro-2H-indazolyl)$_3$]ZnMe and [η^3-HB(3-^{t}Bupz)(3,5-$(CF_3)_2$pz)$_2$]-$ZnOSiMe_3$ and serve as structural models for activated and ground-state configurations of the metal ions during the polymerization reaction. The molecular structure of *meso*-lactide is also reported. These results are compared with polymerizations of lactide by other coordinate catalysts.

Introduction

Arguably the greatest advances in organometallic chemistry within the past decade have come in the field of single-site metal catalysis for olefin polymerization,[1] ring-opening metathesis polymerization, ROMP,[2] and α-olefin-carbon monoxide co-polymerization.[3] For each of the above the development of well-defined organometallic catalyst precursors has led to control of the rate and stereochemistry of polymerization as well as to control of polymer microstructure and molecular weight distribution. By contrast the polymerization reactions leading to polyesters and polyalkene oxides, namely polyoxygenates, have received little attention. These are currently produced by rather ill-defined processes involving so-called coordinate catalysts. For example, Union Carbide employ a heterogeneous calcium amide-alkoxide catalyst system for the polymerization of ethylene- and propylene-oxide[4] and tin(II) octoate or $Al(acac)_3$ are commonly employed in the polymerization of lactide to give polylactide, PLA.[5] The exact nature of the active site is not known nor are details of the ring-opening event understood (established). We reasoned that single-site discrete metal alkoxide complexes of formula L_nM-OR should be excellent catalyst precursors.[6]

* Current address: Newman and Wolfrom Laboratories, the Ohio State University, 100 W. 18th Avenue, Columbus, OH 43210.

(1) (a) Jordan, R. H. *Adv. Organomet. Chem.* **1991**, *32*, 325−387. (b) Ewen, J. A. *J. Am. Chem. Soc.* **1984**, *106*, 6355−6364. (c) Brintzinger, H. H.; Fischer, D.; Mulhaupt, R.; Rieger, B.; Waymouth, R. M. *Angew. Chem., Int. Ed. Engl.* **1995**, *34*, 1143−1170. (d) Coates, G. W.; Waymouth, R. M. *Science* (Washington, D. C.) **1995**, *267*, 217−219. (e) Shapiro, P. J.; Schaeffer, W. P. Labinger, J. A.; Bercaw, J. E.; Cotter, W. D. *J. Am. Chem. Soc.* **1994**, *116*, 4623−4640. (f) Scollard, J. D.; McConville, D. H.; Payne, N. C.; Vitall, J. J. *J. Am. Chem. Soc.* **1996**, *118*, 10008−10009. (g) *Chem. Rev.* **2000**, *100*, April issue.

(2) (a) Schrock, R. R. *Acc. Chem. Res.* **1990**, *23*, 158−165. (b) Schrock, R. R. *Polyhedron* **1995,** *14,* 3177−3195; (c) Lynn, D. M.; Kanoaka, S.; Grubbs, R. H. *J. Am. Chem. Soc,* **1996**, *118*, 784−7980. (d) Week, M.; Schwab, P.; Grubbs, R. H. *Macromolecules* **1996**, *29*, 1789−1793. (e) Bell, A. *J. Mol. Catal.* **1992**, *76*, 165−180. (f) Grubbs, R. H. *J. M. S. Pure Appl. Chem.* **1996**, *A31*, 1829−1833.

(3) (a) Sen, A. *Acc. Chem. Res.* **1993**, *26*, 303−310. (b) Drent, E.; Budzelar, P. H. *Chem. Rev.* **1996**, *96*, 663−681. (c) Rix, F. C.; Brookhart, M.; White, P. S. *J. Am. Chem. Soc.* **1996**, *118*, 4746−4764.

(4) (a) Reichle, W. T. (Union Carbide). U.S. Patent 4,667,013, 1987. (b) Goeke, G. L.; Park, K.; Karol, P. J.; Mead, B. (Union Carbide). U.S. Patent 4,193,892, 1980.

(5) (a) Duda, A.; Penczek, S. *Macromolecules* **1990**, *23*, 1636−1639. (b) Nijenhuis, A. J.; Grijpma, D. W.; Pennings, A. J. *Macromolecues* **1992**, *25*, 6419−6424. (c) Kricheldorf, H. R.; Beri, M.; Schmarnagl, N. *Macromolecules* **1988**, *21*, 286−293. (d) Kowalski, A.; Duda, A.; Penczek, S. *Macromolecules* **1998**, *31*, 2114−2122.

(6) For a preliminary communication of a part of this work, see: Chisholm, M. H.; Eilerts, N. W. *Chem. Commun.* **1996**, 853−854.

10.1021/ja002160g CCC: $19.00
Published on Web 11/17/2000

A list of requirements can be made for this class of compounds. (1) The metal should be redox-inactive and inert to β-hydrogen atom abstraction from the growing alkoxide polymer chain, otherwise side reactions could lead to chain termination with loss of catalytic activity. (2) The inorganic template L_nM should be inert with respect to ligand scrambling, otherwise by intermolecular exchange oligomeric alkoxides may be formed. These would then offer no advantages of single-site catalysis and would be akin to catalysis by alkoxides of Al(3+)[5c,d] or La(3+).[7] (3) The alkoxide ligand in the L_nMOR complex should be labile to alcohol exchange and insertion reactions with C−X multiple bonds. By such reactions chain transfer and functionality can be built into the polymer. (4) Finally, the metal ions and ligands should be inexpensive, colorless, odorless, and biologically benign since trace quantities of the catalyst may ultimately be incorporated into the polymer.[8]

For the above reasons the metal ions Mg^{2+}, Ca^{2+}, and Zn^{2+} are particularly attractive. They are, however, kinetically labile and may readily enter into ligand scrambling as is well-known for the Schlenk equilibrium. Accordingly, we have selected to use bulky tripodal ligands based on substituted trispyrazolyl borates which, as Parkin has shown, may be designed to stabilize metal−alkyl or metal−hydroxide species as in $HB(3\text{-}^tBupz)_3MX$ compounds, where M = Mg, Zn and X = alkyl or OH.[9]

Before we present our results, which represent our initial foray into this field of ROP, we should acknowledge the pioneering work of Inoue and co-workers with (porphyrin)AlX[10] and (porphyrin-Me)ZnX catalyst precursors[11] for the ring-opening polymerizations of epoxides and lactones, the subsequent work of Spassky,[12] and most recently, Coates with related (salen)-AlX compounds.[13] Conceptually, these are related to single-site catalysts described above although the use of the planar porphyrin or salen ligand does not endear itself to cis-substrate uptake. Indeed, there is considerable evidence that the (porphyrin)AlX chemistry proceeds by a reaction pathway that is bimolecular in metal complex[14] and involves backside attack[15] rather than a cis-migratory insertion. The use of the tripodal trispyrazolyl borate ligands endears itself to uptake of substrate at a cis position to the growing polymer chain. We shall comment specifically on the similarities and differences that emerge from our work with Mg and Zn versus the earlier work with planar tetradentate ligands bound to Al.

Results and Discussion

Syntheses of Trispyrazolylborate and Trisindazolylborate Magnesium and Zinc Alkoxides. The synthesis follows directly from the pioneering work of Parkin et al.[9] For magnesium the metathetic reaction between $MgEt_2$ and the thallium(I) trispyrazolylborate or trisindazolylborate yields the magnesium alkyl complexes LMgEt. The TlEt, which is presumably formed, decomposes to Tl metal. It is essential that the pyrazolyl or indazolyl ligand has sufficient steric impedance to shut down the Schlenk equilibrium which would subsequently lead to $MgEt_2$ and $(\eta^3\text{-L})_2Mg$. The use of the 3-^{t}Bupz group is well-known to prevent this and leads to monomeric species. A subsequent alcoholysis reaction, eq **1**, leads to monomeric

$$(\eta^3\text{-L})MgEt + ROH \xrightarrow[\text{benzene}]{25\ ^\circ C} (\eta^3\text{-L})MgOR + C_2H_6 \quad (1)$$

alkoxides in the case of magnesium. We have principally used the ethoxide (R = Et), but *tert*-butoxide and phenoxide can be made in this way. A molecular weight determination on the ethoxide in benzene confirmed its monomeric nature in solution.

The related $(\eta^3\text{-L})ZnEt$ complexes can be prepared in the same manner from the reaction between $ZnEt_2$ and the Tl(I) salts.[19d] The Zn−Et bond in $(\eta^3\text{-L})ZnEt$ complexes is kinetically inert to alcoholysis with ^{t}BuOH and EtOH. The preparation of the Me_3SiO complexes have been previously reported[19d] by reactions between $(\eta^3\text{-L})ZnH$ and Me_3SiOH or by metathetic exchange reactions between $(\eta^3\text{-L})ZnCl$ and $KOSiMe_3$ in benzene. The $(\eta^3\text{-L})ZnCl$ compounds can be prepared from the reactions between $ZnCl_2$ and either the potassium or thallium pyrazolyl/indazolyl borates. Also the OAr complexes can be prepared[16] by the reactions between $((\eta^3\text{-L})ZnOH$ and HOAr.

The C_3-symmetric indazolylborates used in this work were first reported by Tolman.[17] We have mostly worked with those derived from camphor and menthone. We have also noted reactions involving $(\eta^3\text{-L})ZnCl$ compounds may proceed differently with sodium and potassium siloxides in some cases (see Experimental Section).

We have investigated routes to trispyrazolyl borates having different pyrazolyl ligands. It would, for example, be desirous to have access to ligands of the type $HB(3^tBupz)(3\text{-R*pz})_2^-$ wherein appropriate bulk and chirality can be introduced with an optically active group R*. However, the potassium salts of such compounds have proved labile to pyrazolyl group exchange of the type shown in eq **2**.[18]

$$K(3\text{-}^tBupz)(3\text{-Rpz})_2\ BH \underset{\text{benzene}}{\overset{25\ ^\circ C}{\rightleftharpoons}} K(3\text{-}^tBupz)_{3-n}(3\text{-Rpz})_nBH \quad (2)$$

where $n = 0-3$.

Since the potassium salts are involved in the preparation

(7) (a) McLain, S. J.; Ford, T. M.; Drysdale, N. E. *Polym. Prepr. (Am. Chem. Soc. Div. Polym. Chem.)* **1992**, *33(2)*, 463−464. (b) McLain, S. J.; Ford, T. M.; Drysdale, N. E.; Jones, N.; McCord, E. F.; Shreeve, J. L.; Evans, W. J. *Polym. Prepr. (Am. Chem. Soc. Div. Polym. Chem.)* **1994**, *35(2)*, 534−535.

(8) PLAs and functionalized PLAs may be used as drug-delivery reagents and in tissue engineering: (a) Hrkash, J. S.; Ou, J.; Lotan, N.; Langer, R. *ACS Symp. Ser.* **1996**, *627*, 93−102. (b) Mooney, D. J.; Baldwin, D. F.; Suh, N. P.; Vacanti, J. P.; Langer, R. *Biomaterials* **1996**, *17*, 1417−1422. (c) Hubbel, J. A.; Langer, R. *Chem. Eng. News* **1995**, *73*, 42−54. (d) Moondy, D. J.; Breur, C.; McNamara, K.; Vacanti, J. P.; Langer, R. *Tissue Eng.* **1995**, *1*, 107−118.

(9) (a) Han, R.; Parkin, G. *Organometallics* **1991**, *10*, 1010−1020. (b) Han, R.; Parkin, G. *J. Am. Chem. Soc.* **1992**, *114*, 748−757.

(10) (a) Inoue, S.; T. Aida, T. *Macromolcules* **1981**, *14*, 1166−1169. (b) Sugimoto, H.; Aida, T.; Inoue, S. *Macromolecules* **1990**, *23*, 2869−2875. (c) Aida, T.; Inoue, S. *Macromolecules* **1981**, *14*, 1162−1166. (d) Sugimoto, H.; Kawamura, C.; Kuroki, M.; Aida, T.; Inoue, S. *Macromolecules* **1994**, *27*, 2012−2018. (e) Aida, T.; Inoue, S. *Chem. Technol.* **1994**, 28−35.

(11) Atanabe, Y.; Aida, T.; Inoue, S. *Macromolecules* **1990**, *23*, 2612−2617.

(12) Spassky, N.; Wisniewski, M.; Pluta, C.; LeBorgne, A. *Macromol. Chem. Phys.* **1996**, *197*, 2627−2637; Wisniewski, M.; LeBorgne, A.; Spassky, N. *Macromol. Chem. Phys.* **1997**, *198*, 1227−1238.

(13) (a) Coates, G. W.; Ovitt, T. M. *J. Am. Chem. Soc.* **1999**, *121*, 4072−4073. (b) Cheng, M.; Attygalle, A. B.; Lobkovsky, E. B.; Coates, G. W. *J. Am. Chem. Soc.* **1999**, *121*, 11583−11584.

(14) Shimasaka, K.; Aida, T.; Inoue, S. *Macromolecules* **1987**, *20*, 3076−3080.

(15) Watanabe, Y.; Tasuda, T.; Aida, T.; Inoue, S. *Macromolecules* **1992**, *25*, 1396−1400.

(16) Walz, R.; Weis, K.; Ruf, M.; Vahrenkamp, H. *Chem. Ber./ Recueil* **1997**, *130*, 975.

(17) (a) LeCloux, D. D.; Tokar, C. J.; Osawa, M.; Houser, R. P.; Keyes, M.. C.; Tolman, W. B. *Organometallics* **1994**, *13*, 3, 2855−2866. (b) LeCloux, D. D.; Tolman, W. B. *J. Am. Chem. Soc.* **1993**, *115*, 1153−1154.

(18) Chisholm, M. H.; Iyer, S. S.; Streib, W. E. *New J. Chem.* **2000**, *24*, 393−398.

(19) (a) Gorrell, I. B.; Looney, A.; Parkin, G. *J. Chem. Soc., Chem. Commun.* **1990**, 220−222. (b) Gorrell, I. B.; Looney, A.; Parkin, G.; Rheingold, A. L. *J. Am. Chem. Soc.* **1990**, *112*, 4068. (c) Han, R.; Gorrell, I. B.; Looney, A.; Parkin, G. *J. Chem. Soc., Chem. Commun.* **1991**, 717−719. (d) Looney, A.; Han, R.; Gorrell, I. B.; Cornebise, M.; Yoon, K.; Parkin, G. *Organometallics* **1995**, *14*, 274.

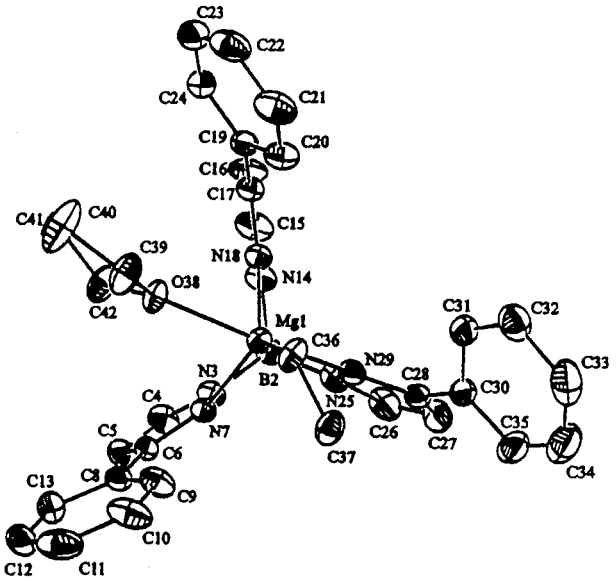

Figure 1. OTREP drawing of [η^3-HB(3-phenylpyrazolyl)$_3$]Mg(CH_2-CH_3)(THF), showing the atom numbering scheme. Atoms are drawn at 50% probability. This view of the molecule is looking down the magnesium boron axis with the THF molecule and the ethyl group coming out of the plane of the paper. Hydrogen atoms have been omitted for clarity.

of the Tl(η^3-Bupz)$_3$BH complexes, our lack of success in suppressing the labile equilibrium **2** has thwarted progress in this area with the following exception. We were able to prepare K(3,5-$(CF_3)_2$pz)$_2BH_2$ and convert this to K(3,5-$(CF_3)_2$pz)$_2$(3-^{t}Bupz)BH, and this "2:1"-trispyrazolylborate does not enter into reaction **2**. By the use of this potassium salt, we prepared the complex [η^3-HB(3-^{t}Bupz)(3,5-$(CF_3)_2$pz)$_2$]ZnOSiMe_3, and its complete synthesis and characterization are given in the Experimental Section.

Structural Studies. Although we are confident (on the basis of the prior structural studies of Parkin[9] and our molecular weight determination of [η^3-HB(3-^{t}Bupz)$_3$]MgOEt in benzene) of the monomeric nature of the (η^3-L)MgOR complexes in solution, we have not been able to obtain crystals suitable for a single-crystal X-ray structural determination. However, to gain insight into the stereochemistry of the ligand and metal centers, we have undertaken structural studies of related complexes. We have also obtained the single-crystal and molecular structure of [η^3-HB(3-^{t}Bupz)(3,5-$(CF_3)_2$pz)$_2$]Zn(OSiMe_3).

[η^3-HB(3-Phpz)$_3$]MgEt(THF). By replacing the bulky ^{t}Bu group by the phenyl at the 3-position of the pyrazolyl one opens up access to the metal center. The structure of [η^3-HB(3-Phpz)$_3$]-MgEt(THF) was therefore undertaken with a view to providing insight into the coordination geometry where a substrate was bound to (η^3-L)M(OP), where OP represents the oxygen-bound terminus of the growing polymer P or, in the initiation step, OP = OR of the single-site catalyst precursor. The structure of the magnesium ethyl complex is shown in Figure 1 and the central N_3MgO(C) unit is shown in Figure 2. Selected bond distances and bond angles are given in Table 1.

The central skeleton (Figure 2) may be described as a distorted trigonal bipyramidal structure wherein two pz nitrogen atoms, N(18) and N(7), occupy equatorial positions (Mg−N (eq) = 2.182(3) Å). The other pz nitrogen, N(29) and the oxygen of the THF are axial (Mg−N(ax) = 2.286(1) Å, Mg−O = 2.201(1) Å, and N(ax)−Mg−O = 160.5(1)). The O−Mg−C angle is 93.6(1)°. The bond distances in the present five-coordinate complex are all slightly longer than those reported

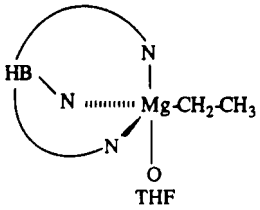

Figure 2. The central MgN_3OC skeleton of the [η^3-HB(3-Phpz)$_3$]MgEt-(THF) molecule, showing the pseudotrigonal bipyramidal structure.

Table 1. Selected Bond Distances (Å) and Angles (deg) for [η^3-HB(3-phenylpyrazolyl)$_3$]Mg(CH_2CH_3)(THF)

A	B	Distance
Mg1	N7	2.182(3)
Mg1	N18	2.182(3)
Mg1	C36	2.155(3)
Mg1	O38	2.201(1)
Mg1	N29	2.286(1)

A	B	C	angle
N7	Mg1	N18	93.1(1)
N7	Mg1	C36	136.3(1)
N7	Mg1	N29	80.8(1)
N7	Mg1	O38	83.0(1)
N18	Mg1	C36	130.1(1)
N18	Mg1	O38	84.2(1)
N18	Mg1	N29	85.0(1)
N29	Mg1	C36	105.6(1)
N39	Mg1	O38	160.5(1)
O38	Mg1	C36	93.6(1)

by Parkin for [η^3-HB(3,5-Me_2pz)$_3$]MgR, where R = Me and CH_2SiMe_3,[9] as expected for an increase in the coordination number of the metal from four to five. Also, for a tripodal ligand at a pseudotrigonal bipyramidal center, the coordination of the trispyrazolyl borate ligand at two equatorial and one axial sites is to be expected. The Mg−Et and Mg−THF bonds must therefore occupy equatorial and axial sites. On the basis of the known tendency for the strongest ligand to occupy the equatorial site it is not surprising to find that the THF ligand is axial. Thus, it is not unreasonable to suppose that for an (η^3-L)MgOR complex the association of substrate would occur initially so that it assumed an axial site adjacent to OR or OP, where O is the oxygen of the growing polymer chain P. A cis-migratory insertion is favored by the close proximity of the cis ligands in axial−equatorial sites and after ring-opening the oxygen atom of the bound substrate would become the oxygen of the new OP ligand and the N_3MgO moiety would once again adopt the pseudotetrahedral geometry.

Tris[(7*R*)-^{i}Pr-(4*R*)-Me-4,5,6,7-tetrahydro-2H-indazolyl]-borate Methyl Zinc. A view of this C_3-symmetric molecule is given in Figure 3. This view is almost looking down the C−Zn bond and shows the helical pitch involving the three ^{i}Pr ligands which are projected toward the Zn−CH_3 moiety with a clockwise twist. The cone angle of this ligand is calculated to be 294°. For comparison, the cone angles of η^3-HB(3,4,5,-H-pyrazolyl)$_3$borate, η^3-HB(3,5-Me_2pz)$_3$ and η^3-HB(3-^{t}Bupz)$_3$ have been estimated to be 184, 224, and 244°, respectively.[9] Selected bond distances and angles are given in Table 2.

The Zn−N bond distances, 2.09(1) Å (ave) are very similar to Zn−N = 2.03 Å (ave) reported by Tolman for the related chloride. Quite possibly, the somewhat longer Zn−N distances in the present molecule reflect the relative donating properties of CH_3^- relative to Cl^- and the subsequent Lewis acidity of the metal center. The Zn−C(methyl) distance of 1.965(5) Å compares well with those reported by Parkin for related η^3-

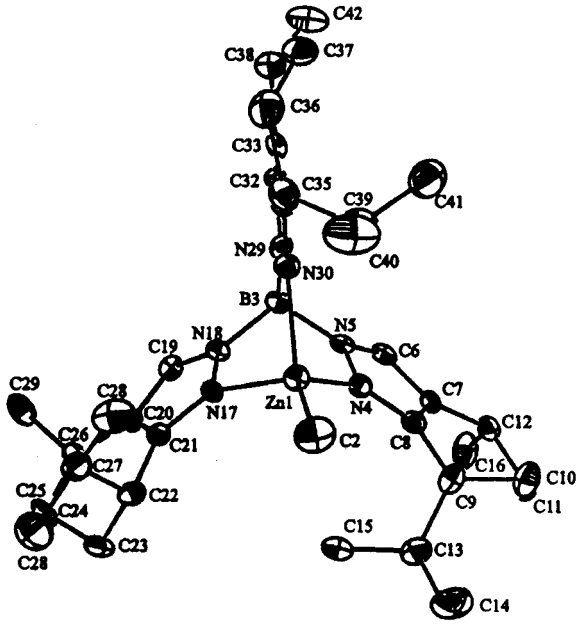

Figure 3. An ORTEP drawing of [tris{(7*R*)-isopropyl-(4*R*)-methyl-4,5,6,7-tetrahydro-2H-indazolyl}borate]zinc(methyl) giving the atom number scheme and showing the C_3-symmetric structure. Hydrogen atoms have been omitted for clarity.

Table 2. Selected Bond Distances (Å) and Angles (deg) for [Tris{(7*R*)-isopropyl-(4*R*)-methyl-4,5,6,7-tetrahydro-2H-indazolyl}-borate]zinc(methyl)

A	B	distance
Zn1	C2	1.965(5)
Zn1	N4	2.099(4)
Zn1	N17	2.086(4)
Zn1	N30	2.088(4)

A	B	C	angle
N4	Zn1	N17	87.8(2)
N4	Zn1	C2	126.2(2)
N4	Zn1	N30	89.9(1)
N17	Zn1	N30	92.9(1)
N17	Zn1	C2	122.4(1)
N30	Zn1	C2	126.6(1)

trispyrazolylborate zinc methyl complexes.[19] It is interesting to note that, despite the similar size of Mg^{2+} and Zn^{2+} ions in related coordination complexes, for η^3-trispyrazolyl M−C(alkyl) complexes the Zn−C bonds are significantly shorter than their Mg−C(alkyl) counterparts. We attribute this to the softer nature of zinc. The η^3-LZn−C(alkyl) bond is more covalent and less reactive toward H_2O and ROH substrates.

If we take the present structure of (η^3-L*)$ZnCH_3$ to model the resting state for the catalyst (η^3-L*)ZnOP, then substrate uptake would generate a five-coordinate metal center with the substrate in an axial-site adjacent to two cis-chiral chelating arms of the tripodal ligand. The growing polymer chain would again initially occupy an equatorial position. The influence of the third chiral pz group in the axial site would thus seem to be small, at least with respect to substrate uptake. It would, however, exert an influence on its cis-OP ligand, and this in turn could assist in the cis-migratory insertion step wherein the five-coordinate activated complex [reactive intermediate] returned to the C_3-symmetric η^3-L*MOP complex.

[η^3-HB(3-^{t}Bupz)(3,5-$(CF_3)_2$pz)$_2$]ZnOSiMe$_3$, 5. The molecular structure of compound **5** is shown in Figure 4 and selected bond distances and bond angles are given in Table 3. The most important feature of the molecular structure is that it confirms

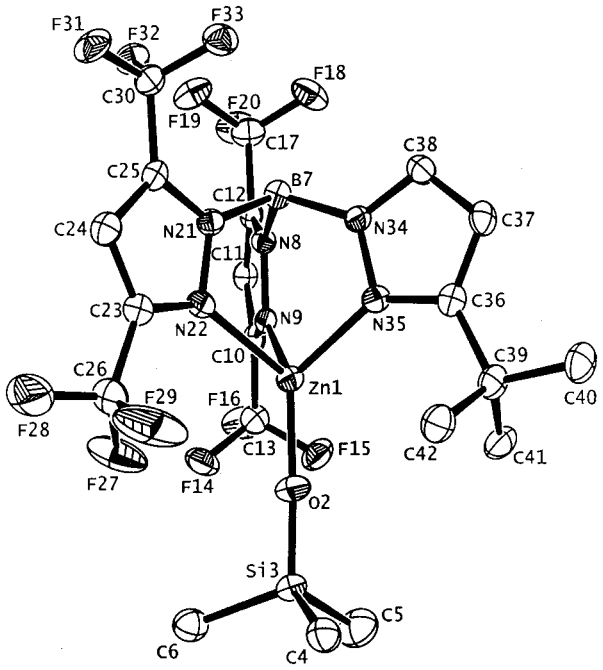

Figure 4. An ORTEP drawing of [η^3-HB(3-^{t}Bupz)(3,5-$(CF_3)_2$pz)$_2$]-ZnOSiMe$_3$, **5**, giving the atom number scheme used in the Table.

Table 3. Selected Bond Distances (Å) and Angles (deg) for[η^3-HB(3-^{t}Bupz)(3,5-$(CF_3)_2$Pz)$_2$]ZnOSiMe$_3$, **5**

A	B	distance
Zn(1)	O(2)	1.792(2)
Zn(1)	N(9)	2.084(3)
Zn(1)	N(22)	2.115(3)
Zn(7)	N(35)	2.022(3)
Zn(43)	O(44)	1.795(2)
Zn(43)	N(51)	2.098(3)
Zn(43)	N(64)	2.105(3)
Zn(43)	N(77)	2.017(3)

A	B	C	angle
O(2)	Zn(1)	N(9)	119.3(1)
O(2)	Zn(1)	N(22)	125.2(1)
O(2)	Zn(1)	N(35)	128.3(1)
N(9)	Zn(1)	N(22)	87.9(1)
N(9)	Zn(1)	N(35)	94.6(1)
N(22)	Zn(1)	N(35)	90.0(1)
O(44)	Zn(43)	N(51)	120.5(1)
O(44)	Zn(43)	N(64)	121.2(1)
O(44)	Zn(43)	N(77)	131.8(1)
N(51)	Zn(43)	N(64)	87.5(1)
N(51)	Zn(43)	N(77)	93.5(1)
N(64)	Zn(43)	N(77)	90.8(1)

the monomeric nature of the compound. The Zn−O−Si angle is nearly linear 175(1) ° (ave) and the Zn−N distances fall into two groups with those associated with the 3-^{t}Bupz ligand being nearly 0.1 Å (ave) shorter than those associated with the 3,5-$(CF_3)_2$pz ligands. This is understandable in terms of basicity since the CF_3 groups are electron withdrawing while ^{t}Bu is a good σ-donor. It is, however, interesting to see this structural effect, and since there are two crystallographically different molecules of compound **5** in the unit cell, one sees this effect in both molecules. Only one of the molecules is shown in Figure 3, but an inspection of the structural data presented in Table 3 provides a reassurance of their similarity. The structure of [η^3-(3-^{t}Bupz)$_3$BH]ZnOSiMe$_3$ was also determined, and structural data are reported in the Supporting Information.

***meso*-Lactide.** It has been reported in the literature that *meso*-lactide polymerizes at a slower rate than L-lactide and *rac*-

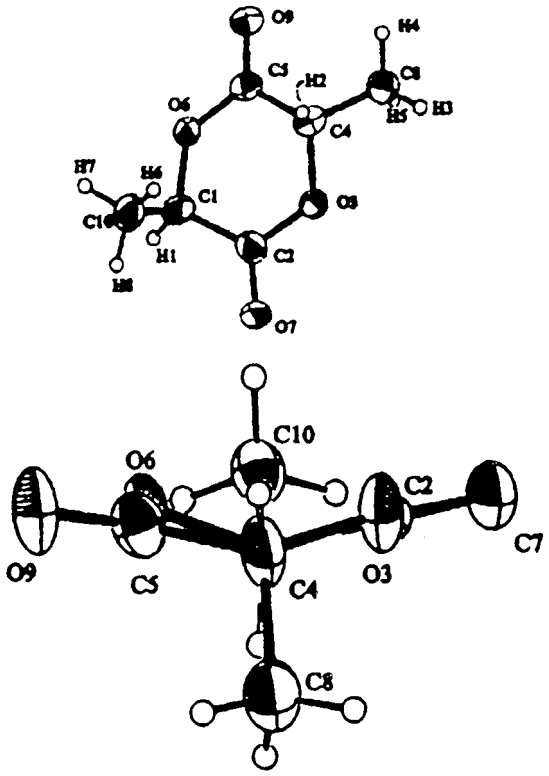

Figure 5. Two ORTEP drawings of *meso*-dilactide, showing the atom number scheme. Atoms are drawn at 50% probability. The side-on view (bottom) depicts the distorted flat structure of the molecule looking down the C4−C1 axis; this is the most stable form of the molecule according to PCMODEL calculations (see text).

lactide, and it was suggested that this is because of the difference in the stability of the *meso* and L- and D-lactide in the ground-state.[20] As shown below L- and D-lactide have two chiral carbons of the same handedness, either *S,S* or *R,R*, and the two Me groups occur on the same side of the six-membered ring, whereas the *meso*-diastereomer has two stereocenters of opposite chirality, *R,S*, and the methyl groups lie on opposite sides of the six-membered ring.

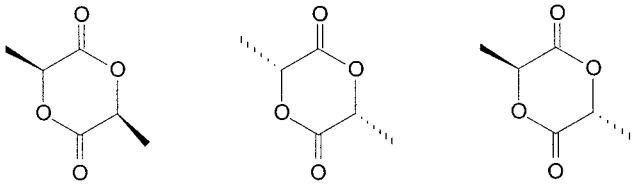

L-Lactide (S,S) D-Lactide (R,R) Meso-Lactide(S,R)

Since we have found preferential polymerization of *meso*-lactide over L-lactide and *rac*-lactide, we determined the molecular structure of *meso*-lactide in the solid-state. A view of the molecule is given in Figure 5 and selected bond distances and bond angles are given in Table 4.

The bond distances and bond angles are very similar to those reported previously for L- and D-lactide as determined from a single-crystal structure of *rac*-lactide.[21] From the view shown in Figure 5, it is evident that the ground-state configuration of the molecule is between a twist-boat and a planar structure, and thus the six-membered ring is close to planar. PC MODEL[22] calculations reveal that the planar structure is favored, at least in part, because the lone pairs of the two oxygen atoms of each ester group repel each other.

Table 4. Bond Distances (Å) and Angles (deg) for *meso*-Lactide

A	B	distance	A	B	distance
O3	C2	1.345(6)	O3	C4	1.467(9)
O6	C1	1.459(8)	O6	C5	1.346(6)
O7	C2	1.186(9)	O9	C5	1.210(8)
C1	C2	1.508(5)	C1	C10	1.473(9)
C4	C5	1.520(3)	C4	C8	1.492(7)

A	B	C	angles	A	B	C	angles
C2	O3	C4	120.9(3)	C1	O6	C5	122.0(2)
O6	C1	C2	112.8(4)	O6	C1	C10	111.0(6)
C2	C1	C10	112.0(3)	O3	C2	O7	119.4(3)
O3	C2	C1	119.6(6)	O7	C2	C1	120.8(5)
O3	C4	C5	111.2(4)	O3	C4	C8	106.9(4)
C5	C4	C8	112.5(4)	O6	C5	O9	118.8(2)
O6	C5	C4	119.2(6)	O9	C5	C4	122.0(5)

PC MODEL calculations using the coordinates of the molecular structure of the *meso*- and *rac*-lactides as input data were performed. The relative minimized energies (MMX) for *meso*- and L-lactide are 0.24 and 0.14 kcal mol^{-1}, respectively. CVFF (consistent valence force field) calculations[23] also show that the racemic lactide is 0.4 kcal mol^{-1} more stable than the *meso*-lactide. These calculations support the view that the *meso*-lactide is less stable in the ground-state relative to L- and D-lactide. These small calculated differences in ground-state energies, if they are real, may contribute to the $\Delta\Delta G^{\ddagger}$ values of ring-opening such that *meso* reacts faster than *rac*, although other factors may be equally important.

Catalyst Precursors: General Comments on Reactivity. Although several (η^3-L)M(OR) complexes were prepared and

(20) Kricheldorf, H. R.; Boettcher, C.; Tonnes, K. U. *Polymer* **1992**, *33*, 2817.

(21) Van Hummel, G. J.; Harkema, S.; Kohn, F. E.; Feijen, J. *Acta Crystallogr.* **1982**, *B38*, 1679.

(22) PCModel is derived from several sources. The graphical user interface originally came from MODEL, written by C. Still of Columbia University. It has been extensively modified for PCMODEL for Windows. The MODEL code originally ran on a DEC Vax computer and is still supported by Kosta Steliou of Boston University. MODEL was ported to the IBM-PC and renamed PCMODEL by M. Mark Midland, University of California, Riverside, J. J. Gajewski of Indiana University, Kosta Steliou of Boston University, and K. E. Gilbert of Serena Software. PCMODEL was then ported to the Macintosh, Silicon Graphics, and Sun workstations by K. E. Gilbert, J. J. Gajewski, and T. W. Kreek of Indiana University. The current version of PCMODEL for Windows and for the Apple Macintosh was written by K. E. Gilbert. The force field used in PCMODEL is called MMX and is derived from MM2 (QCPE−395, 1977) force field of N. L. Allinger, with the pi-VESCF routines taken from MMP1 (QCPE−318), also by N. L. Allinger. The pi-VESCF routines were modifed for open-shell species by J. McKelvey of Kodak, while improvements to the heat of formaton calculations were done by J. J. Gajewski. MMX increased the number of atom types for the MM2 force field, added the ability to handle transition metals and transition states, and increased the number of parameters included in the database. These changes were made by J. J. Gajewski and K. E. Gilbert. For references regarding molecular mechanics see (a) Burkert, U.; Allinger, N. L. *Molecular Mechanics*; ACS Monograph Series 175; American Chemical Society: Washington, DC. (b) Clark, T. *A Handbook of Computational Chemistry: A Practical Guide to Chemical Structure and Energy Calculations*; John Wiley and Sons: New York, 1985. (c) *Reviews in Computational Chemistry*; Lipkowitz, K., Boyd, D. B, Eds.; VCH: New York, 1990. (d) *Journal of Computational Chemistry*; Allinger, N. L., Ed.; PCMODEL version 7 is available from Serena Software, Box 3076, Bloomington, IN 47402-3076, Telephone: (812) 333-0823, FAX: (812) 332-0877, E-mail: gilbert@serenasoft.com.

(23) The CVFF or consistent valence force field was originally created for modeling proteins and peptides and has been extended to handle more general systems having similar functional groups. CVFF can be performed using the Discover or INSIGHT program marketed by Biosym/MSI, 9685 Scranton Road, San Diego, CA 92121-3752. For more information on force field see (a) Ermer, O. Calculation of Molecular Properties using Force Fields. Applications in Organic Chemistry. *Struct. Bonding* **1976**, *27*, 161−211. (b) Hagler, A. T. Theoretical Simulation of Conformation, Energetics, and Dynamics of Peptides. In *Conformation of Biology and Drug Design, The Peptides*; Meienhofer, J., Ed.; Academic Press: New York, 1985; Vol. 5, pp 213−299.

their reactivity was surveyed, only the reactions of [η^3-HB(3-^{t}Bupz)$_3$]Zn(OSiMe$_3$), **1**, [η^3-HB((7*R*)-^{i}Pr-(4*R*)-Me-4,5,6,7-tetrahydro-2H-indazolyl)$_3$] Zn(OSiMe$_3$), **2**, [η^3-HB(3-^{t}Bupz)$_3$]-MgOEt, **3**, [η^3-HB((7*R*)-^{i}Pr-(4*R*)-Me-4,5,6,7-tetrahydro-2H-indazlyl)borate]MgOPh, **4**, and [η^3-(3-^{t}Bupz)(3,5-(CF$_3$)$_2$pz)$_2$BH]-ZnOSiMe$_3$, **5**, with lactide will be described in detail in this work. The following general comments are, however, worthy of note as these are elaborated upon in detail or will be described subsequently.

1. The magnesium compounds are notably more reactive than the zinc complexes. This has both positive and negative implications. The magnesium catalyst precursors are extremely water- and air-sensitive, and the presence of water leads to deactivation of the catalyst. Under rigorously dry conditions, the magnesium catalyst systems are among the most active reported to date being only slightly less active that lanthanide alkoxides reported by workers at DuPont.[7]

2. The zinc complexes, while slower than their related magnesium counterparts, are more tolerant. The zinc trimethylsiloxides are even inert to air in the solid state for a period of a few days. In solution the zinc complexes will polymerize episulfides and copolymerize L-lactide and 3*S*,6*S*-dimethylmorpholine-2,5-dione (85:15 mixture), whereas the magnesium catalysts systems are killed by episulfides and morpholine 2,5-dione. [This is not the subject of this report and will be discussed elsewhere.]

3. Neither the magnesium nor the zinc complexes will polymerize propylene oxide at ambient temperatures although steric access to the metal center is apparent from NOE studies which implicate reversible binding.

4. Polymerization of lactone has been observed as has insertion of CO_2 into the M−OR bond to generate MO_2COR (as judged by ^{13}C NMR spectroscopy). Insertion of CO_2 into the ZnOR bond requires heating to 60 °C and pressure ≥10 atm. The result is noteworthy, however, in light of the recent work of Darensbourg[24] and Coates[25] on the copolymerization of CO_2 and alkene oxides.

5. The introduction of trifluoromethyl groups, as present in the complex [η^3-HB(3-^{t}Bupz)(3,5-(CF$_3$)$_2$pz)$_2$]ZnOSiMe$_3$, suppresses the rate of lactide polymerization to the point where it is nearly inactive at room temperature.

We describe below our specific studies of lactide polymerizations by the precursor complexes **1**, **2**, **3**, **4**, and **5** defined above.

Mechanism of Ring-Opening of Lactide. Ring-opening of lactide can occur by either acyl cleavage or ether cleavage (See Scheme 1). In the former process the carbonyl group is attacked, leading to an ester end group and an alkoxy group bound to the metal, while in the latter the end group is an ether and an ester group is bound to the metal. Reactions employing **3** have clearly identified the end group as an ester bearing the original OCH_2CH_3 moiety. The ester OEt group is readily detected by ^{1}H and ^{13}C NMR spectroscopy as the O*C*H_2 ^{1}H and ^{13}C signals for an ester and ether moiety have quite different chemical shifts.[26] In the ^{1}H spectrum the ester methylene protons are at δ 4.18 consistent with acyl cleavage.

Kinetics of ring-opening polymerization have been determined in CD_2Cl_2 and $CDCl_3$ solutions. The reactions have been shown to be first-order in lactide and first-order in metal

Scheme 1

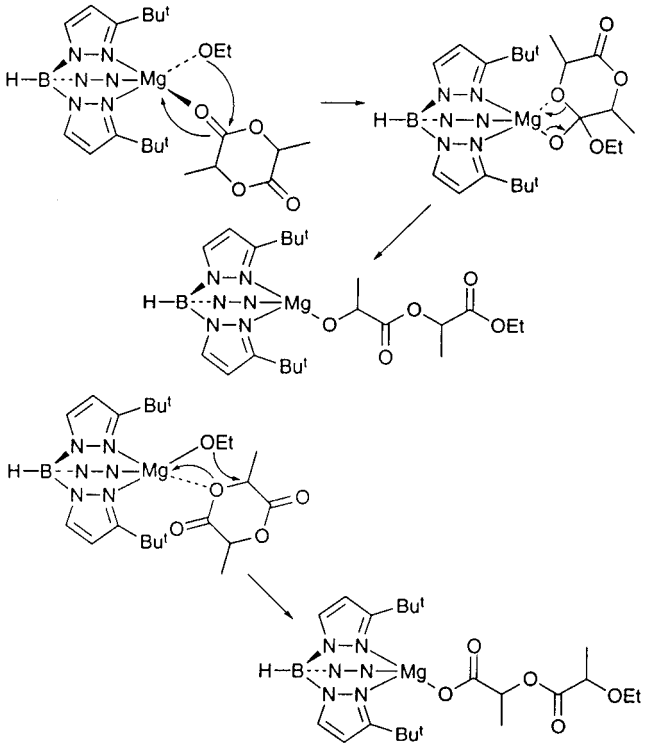

complex. Under pseudo-first-order conditions with a large excess of lactide, $k_{obs} = 7.8 \times 10^{-4}$ min^{-1} and 3.9×10^{-2} min^{-1} for zinc and magnesium complexes having the common ligand L = η^3-HB(3-^{t}Bupz)$_3$. Clearly the zinc complex is a much slower catalyst than the magnesium. The value of $k_{obs} = 1.0 \times 10^{-2}$ min^{-1} for **2** relative to $k_{obs} = 7.8 \times 10^{-4}$ min^{-1} for **1** presumably reflects the importance of the greater steric crowding imposed by the chiral tris-indazolyl ligand which evidently enhances the rate of polymerization.

We attribute the difference in reactivity between related Mg and Zn complexes, that is, **1** and **3**, to the difference in polarity of the M−OR bond. For M = Mg, the metal is more electropositive, and thus the metal has significant $\delta+$, and the alkoxide oxygen, $\delta-$ charge. The metal center thereby activates the ketonic carbon to nucleophilic attack by the attendant OR$^-$ ligand more for M = Mg than for M = Zn which has a more covalent and less highly polarized M−OR bond. This represents one working hypothesis for the interpretation of the observed data and goes a long way in explaining the comparative catalyst activities shown in Table 5. The highest activity is observed for lanthanide alkoxides as reported by workers from DuPont.[7] Of course, Ln(OR)$_3$ species are not single-site catalysts. They are aggregates and often actually oxo alkoxides, Ln$_5$O(OR)$_{13}$.[27]

For polymerizations of L-lactide employing compounds **1** and **3** we observed a linear relationship between molecular weight and the % conversion (See figures in Supporting Information) and the number of polymer molecules which can be calculated from molecular weight and % yield equal to that of the catalyst. The polydispersity (M_n/M_w) remained fairly constant with a PDI within the range 1.1−1.25 to 90% conversion. The PDI increased slightly during the latter parts of the reaction. We attribute this to backbiting or transesterification reactions which start to compete with the polymerization as the polymer molecular weight gets high and the substrate (monomer) concentration is low.

(24) Darensbourg, D. J.; Holtcamp, M. W.; Khamdelwal, B.; Klausmeyer, K. K.; Reibenspies, J. H. *J. Am. Chem. Soc.* **1995**, *117*, 538−539.

(25) Cheng, M.; Lobkovsky, E. B.; Coates, G. W. *J. Am. Chem. Soc.* **1998**, *120*, 11018−11019.

(26) Silverstein, R. M.; Bassler, G. C.; Morill, T. C. *Spectroscopic Identification of Organic Compounds*, 5th ed.; John Wiley and Sons: New York, 1991; p 201 (Appendix 1).

(27) Poncelet, O.; Sartain, W. J.; Hubert-Pfalzgraph, L. G.; Folting, K.; Caulton, K. G. *Inorg. Chem.* **1989**, *28*, 263−267.

Table 5. Summary of Comparative Data for the Polymerization of L-Lactide by Various Coordinate Catalysts

catalyst	conditions	catalyst concentration, M	[monomer]/[catalyst]	*t* to %
$Sn(oct)_2$	dioxane, 120 °C	2.4×10^{-2}	42	50 min, 80
$Sn(oct)_2$	lactide, melt, 110 °C		10 000	4 h, 80
$Zn(^tBuacac)_2$	lactide, melt, 110 °C		10 000	8 h, 80
$Al(O^iPr)_3$	CH_2Cl_2, 100 °C	1	300	3 h, 80
$Ti(OBu^n)_4$	CH_2Cl_2, 100 °C	1	200	24 h, 90
Bu^n_3SnOMe	CH_2Cl_2, 100 °C	1	200	24 h, 95
(TPP)Al(OR)	CH_2Cl_2, 100 °C	1.65×10^{-2}	100	96 h, 90
$Y(OCH_2CH_2NMe_2)_3$	CH_2Cl_2, 25 °C		400	15 min, 90
$HB(^tBupz)_3MgOEt$	CH_2Cl_2, 25 °C	1.1×10^{-2}	500	60 min, 90
$HB(^tBupz)_3ZnOEt$	CH_2Cl_2, 25 °C	1.1×10^{-2}	500	6 d, 90

Table 6. Optical Rotation Data of Polylactides Using Two Different Catalyst Precursors and Two Different Monomers. α_D of L-lactide and Poly(L-lactide) Are −285° and −144°, Respectively

catalyst entry	**2** % conversion[a]	2 α_D of remaining onomer	2 α_D of polymer	**2** % ee[b]	**1** % conversion[a]	1 α_D of remaining monomer	1 α_D of polymer
1	11	+53.0	−10	18.5	17	-0.01	0.01
2	12.9	+41.7	−6.5	14.6	34	0.00	0.00
3	19	+54	−6.8	18.9	40	0.003	0.00
4	27	+44	−10.8	15.4			

[a] % conversion by ^1H NMR. [b] % ee = {α_D (of remaining monomer)/285}*100. **1** = [η^3-HB(3-^{t}Bupz)$_3$]ZnOSiMe$_3$**2** = [η^3-HB((7*R*)-^{i}Pr-(4*R*)-Me-4,5,6,7-tetrahydro-2H-indazolyl)$_3$]ZnOSiMe$_3$.

Diastereoselective and Enantioselective Polymerizations. Polymerization of L-lactide by the magnesium and zinc alkoxide catalyst systems gives poly(L-lactide). No epimerization is observed. The achiral catalyst precursors **1** and **3** show a significant preference for the polymerization of *meso*-lactide over L- and D-lactide in methylene chloride. This is readily seen from ^1H NMR studies of a 1:1 mixture of *meso*:*rac*-lactide in CD_2Cl_2 at 22 °C. (See Figure in Supporting Information) This observation is the opposite of what has been claimed previously and is not reconcilable with the view that the *meso* diastereomer is more stable in the ground state as stated in that work.[20]

Copolymerizations of a 1:1 *meso*:*rac* lactide were also carried out using the chiral zinc and magnesium catalysts **2** and **4** with rather interesting although not readily explainable results. The chiral magnesium complex **4** showed a marked preference for the polymerization of *meso* over *rac* (as did the achiral magnesium complex **3**). In CD_2Cl_2 at −40 °C *meso*-lactide was effectively polymerized, exclusively leaving only unreacted *rac*-lactide. The polymerization of the *meso* was slow at −40 °C and required ∼2 days to go to 90% completion. Examination of the poly(*meso*-lactide) by ^1H and $^{13}C\{^1H\}$ NMR spectroscopy revealed a modest preference for the formation of syndiotactic tetrad sequences, ∼25% more than the Bernoullian statistical distribution.[28] The chiral magnesium catalyst system, **4**, thus shows enhanced diastereoselective polymerization (relative to **3**) but only a modest stereoselectivity.

The copolymerizatioin of a 1:1 mixture of *meso*- and *rac*-lactide by the chiral zinc complex **2** in CD_2Cl_2 revealed that *meso* and *rac* were polymerized at essentially the same rate during the initial phase of the polymerization, that is, over the first 30% of the polymerization. Then the *meso* was consumed faster. This behavior contrasts sharply with the behavior of the related chiral magnesium complex **4** which shows a much more marked diastereoselective preference for the *meso* isomer.

Of course, a chiral catalyst may show pronounced enantioselectivity in its polymerization of *rac*-lactide and there is one such example reported by Spassky[12] who employed a chiral salen Al−OR catalyst system. [This same system was recently employed by Coates[13a] in the polymerization of *meso*-lactide to give the first example of highly (>95%) syndiotactic poly(*meso*-lactide)]. In this work the authors took aliquots of the reaction mixture at different intervals of time and precipitated the polymer. They made the assumption that the molecular weight of the polymer has no effect on the observed optical activity. We felt it worthwhile to establish this and prepared poly(L-lactide) of varying molecular weights and measured the optical activity of the polymers. Indeed, for poly(L-lactide) with $M_w > 6000$ the optical activity remains constant with $\alpha^{22}_D \approx 142°$. However, while this confirms the use of the analytical technique employed by Spassky, the technique is not so useful in our case since our catalyst system shows much lower enantioselectivity in the polymerization of *rac*-lactide. Consequently, we took aliquots from the reaction mixture and quenched with methanol. The optical activity of the solution of lactide over the first 30% of the polymerization was monitored. These data are given in Table 6 and reveal that the chiral complex **2** exhibits a preference for the polymerization of L-(*S*,*S*)-lactide. In **2**, the stereocenters at the ^{i}Pr- and Me-substituted carbon atoms are both *R*. Therefore a right-handed catalyst preferentially chooses the left-handed (*S*,*S*) isomer of the monomer in the ring-opening process. The enantioselectivity is very modest as is evident from the low ee values reported in Table 6.

Concluding Remarks

This work documents the first study of well-defined single-site catalyst precursors for the ring-opening of lactides. The reactions are first-order in catalyst and first-order in substrate. Ring-opening occurs by cis-migratory attack of an alkoxy group on a neighboring carbonyl group to regenerate an alkoxy group of the growing polymer bound to the metal. The polymerizations are living and give relatively low PDIs, ∼1.1−1.3 up to 90% conversion. This indicates that *k* initiation is comparable if not greater than *k* propagation and that transesterification is not significant up to 90% conversion. The magnesium catalyst systems are highly active in showing rapid ring-opening polymerization at room temperature in methylene chloride. The zinc alkoxide systems, although slower, are more tolerant and may prove useful in the preparation of functionalized lactide polymers and copolymers. Changing the nature of the attendant

(28) Chisholm, M. H.; Iyer, S. S.; McCollum, D. G.; Pagel, M.; Werner-Zwanziger, U. *Macromolecules* **1999**, *32*, 963−976.

ligand L in LMOR catalyst precursors can have a marked influence on the rate of polymerization. That introducing electron-withdrawing groups on the pz ligand, that is, as in 3,5-$(CF_3)_2$pz versus 3-^{t}Bupz, suppresses the rate leads us to propose that the more polar the $M^{\delta+}-^{\delta-}OR$ bond the more rapid is the rate of ring-opening. That the more bulky catalyst precursors derived from menthone show faster reactivity relative to the achiral ^{t}Bupz leads us to believe steric crowding also facilitates ring-opening. This could be brought about by crowding in a five-coordinate adduct wherein the O−M−O angle involving the lactide substrate and the oxygen atom of the alkoxy group of the polymer chain becomes smaller, thereby facilitating the migratory attack by the alkoxide on the carbonyl carbon. However, we cannot discount the fact that one pz ligand dissociates with increasing steric encumbrance at the metal center. This work also reports the first examples of a pronounced diastereoselective polymerization of *meso*-lactide in the presence of *rac*-lactide (in contrast to a previous ordering which implicated polymerization of *meso* was slower).[20] As the crystal structure of *meso*-lactide and MMO calculations imply, this may, in part, reflect differences in the ground-state energies of *meso*- and L/D-lactide. However, the marked difference in the diastereoselective polymerization properties of the structurally related chiral zinc and magnesium complexes **2** and **4**, respectively, indicates that we do not really understand the factors that control the ring-opening event. This is true of the porphyrin- and salen-Al alkoxides employed by Inoue,[10,11] Spassky[12] and most recently by Coates.[13a] Indeed, since the completion of this work Coates and co-workers[13b] have communicated that a dimeric zinc alkoxide $[LZn(\mu\text{-}O^iPr)]_2$, where L = the uninegatively charged chelating anionic ligand derived from deprotonation of a 2-((2,6-diisopropylphenyl)amino)-4-((2,6-diisopropylphenyl)imino)-2-pentene, is highly active in the polymerization of lactide at 20 °C and will polymerize *rac*-lactide to give heterotactic PLA (*sisisi*-PLA). The authors conclude that the stereoselectivity arises from end-group control since the catalyst precursors are achiral. It is not readily apparent why the Coates zinc system involving a dimeric precursor should be more active and stereoselective than the monomeric sterically crowded chiral and achiral systems reported here. Also in a recent communication Hillmyer and Tolman[29] described the activity of well-defined dimeric yttrium alkoxides, which, while acting as polymerization catalyst systems for L-lactide, were less reactive than the ill-defined systems employed by the DuPont workers. However, through a systematic study of the development of single-site L_nMOR catalyst precursors for the ring-opening of lactides we should see the emergence of a new class of functionalized polymers and copolymers based on lactide with potentially wide ranging applications in the biomedical field.[8]

Experimental Section

General Considerations. The manipulation of air-sensitive compounds involved the use of anhydrous solvents and dry and oxygen-free nitrogen, employing standard Schlenk line and drybox techniques. Lactide (L- and *rac*-) was purchased from Aldrich and was sublimed twice prior to use. *meso*-Lactide 93% (+ 7% *rac*) was a gift from Mark Hartman, Cargill, Minnesota, and was similarly purified. (Note well: It is important to purify the lactide prior to polymerization experiments as impurities present in unpurified samples can kill the magnesium and zinc catalyst systems reported herein.) $MgEt_2$ was prepared from EtMgCl (Aldrich) and was titrated with a standard HCl solution to determine its concentration prior to use. $ZnCl_2$, TlOAc, $NaOSiMe_3$, and $KOSiMe_3$ were purchased from Aldrich and were used as received. The syntheses of η^3-HB(3-^{t}Bupz)$_3$Tl[30] and [η^3-HB((7*R*)-^{i}Pr-(4*R*)-Me-4,5,6,7-tetrahydro-2H-indazolyl]Tl[17a] and $KH_2B(3,5\text{-}(CF_3)_2pz)_2$[31] followed literature procedures.

Measurements. ^{1}H and $^{13}C\{^1H\}$ spectra were recorded in C_6D_6, CD_2Cl_2, $CDCl_3$, or $C_6D_5CD_3$ solvents on either Varian I-400 or I-500 NMR spectrometers and were referenced internally to the residual protio impurity peaks (C_6D_6 δ 7.15, CD_2Cl_2 δ 5.32, $CDCl_3$ δ 7.24, and $C_6D_5CD_3$ δ 2.09 for ^{1}H, and C_6D_6 δ 128.0, CD_2Cl_2 δ 53.8, $CDCl_3$ δ 77.0, and $C_6D_5CD_3$ δ 20.4 for $^{13}C\{^1H\}$). A pulse delay time of 15 s was employed in NMR studies of the kinetics of polymerization where integrations of polymer and monomer (lactide) were undertaken. ^{19}F NMR spectra were recorded on a Varian I-400 and referenced to external CF_3COOH. IR measurements were performed with a Perkin-Elmer FTIR spectrophotometer. GPC measurements were performed at 25 °C on a Waters 746 gel permeasion chromatograph equipped with a differential refractometer detector using THF as the solvent at a flow rate of 1 mL/min. The column was ultrastyrogel 10^3 Å, and the molecular weights were relative to polystyrene standards. These molecular weights were then corrected according to a universal calibration curve. The optical activity measurements were performed on a Perkin-Elmer 241 Polarimeter equipped with a Na lamp operating at 589 nm with the temperature kept at 22 °C.

[η^3-HB(3-^{t}Bupz)$_3$]ZnOSiMe$_3$, 1. $ZnCl_2$ (0.23 g, 17.1 mmol) was slurried in THF (5 mL), and a solution of η^3-HB(3-^{t}Bupz)$_3$Tl (1.0 g, 17.1 mmol) in THF (10 mL) was added to it. There was an immediate formation of a white precipitate of TlCl. The mixture was stirred for 30 min and filtered through Celite to give a clear solution. Removal of the solvent gave [η^3-HB(3-^{t}Bupz)$_3$]ZnCl (0.71 g, 93%) as a crystalline product which was judged to be >95% pure by ^{1}H NMR spectroscopy and was used without further purification in the next step of the synthesis. ^{1}H NMR (C_6D): 7.26 (d, 1H, J = 1.2 Hz), 5.79 (d, 1H, J = 1.2 Hz), 1.51 (s, 9H).

[η^3-HB(3,^{t}Bupz)$_3$]ZnCl (0.71 g, 16 mmol) dissolved in benzene (10 mL) was added dropwise to $KOSiMe_3$ (0.20 g, 25.7 mmol) with stirring over 10 min. [It seems to be important to add the zinc solution to the solid as attempted reactions employing $KOSiMe_3$ dissolved in benzene failed to give the desired product.] Filtration of the resultant benzene solution through Celite followed by crystallization gave compound **1** as a fine microcrystalline powder (0.75 g, 88% yield). Elemental analysis, found (calcd): C 53.6 (53.7); H 7.49 (7.80); N 15.2 (15.7). ^{1}H NMR (C_6D_6): 7.26 (d, 1H, J = 3 Hz), 5.78 (d, 1H, J = 3 Hz), 1.46 (s, 9H), 1.77 (s, 3H).

[η^3-HB((7*R*)-^{i}Pr-(4*R*)-Me-4,5,6,7-tetrahydro-2H-indazolyl)$_3$]-ZnOSiMe$_3$, 2. The reaction was performed as above for **1** but employing [η^3-HB((7*R*)-^{i}Pr-(4*R*)-Me-4,5,6,7-tetrahydro-2H-indazolyl)$_3$]-ZnCl (0.133 g, 21 mmol) yielding upon crystallization (0.084 g, 58%) of **2**. ^{1}H NMR 7.28 (s, 1H), 3.02 (m, 1H), 2.41 (m, 2H), 1.77 (m, 2H), 1.42 (m, 3H), 1.20 (d, 3H, J = 4.8 Hz), 1.00 (d, 3H, J = 5.4 Hz), 0.82 (d, 3H, J = 5.1 Hz) for the ZnCl complex. For **2**, elemental analysis found (calcd): C 61.5 (61.9), H 8.2 (8.7), N 10.7 (12.0). ^{1}H NMR (C_6D_6) 7.22 (s, 1H), 2.91 (m, 1H), 2.44 (m, 2H), 1.55 (m, 1H), 1.48 (m, 2H), 1.28 (m, 1H), 1.20 (d, 3H, J = 6.9 Hz), 1.01 (d, 3H, J = 6.9 Hz), 0.84 (d, 3H, J = 6.9 Hz), 0.63 (s, CH_3Si, 3H).

[η^3-HB((7*R*)-^{i}Pr-(4*R*)-Me-4,5,6,7-tetrahydro-2H-indazolyl)$_3$]-ZnMe. [η^3-HB((7*R*)-^{i}Pr-(4*R*)-Me-4,5,6,7-tetrahydro-2H-indazolyl)]Tl (1.0 g, 13.6 mmol) was dissolved in THF (10 mL) and cooled to 0 °C. To this solution was added 1 equiv of Me_2Zn (0.68 mL of a 2 M solution in Et_2O). There was an immediate formation of Tl metal which coated the flask. The solution was stirred for 10 min at 0 °C, allowed to warm to room temperature, and stirred for a further 30 min with the aid of a magnetic spin bar. The solution was filtered through Celite to give a clear solution. The solvent was removed under a dynamic vacuum, and the resultant solids were recrystallized from toluene (5 mL) with cooling in a refrigerator at −10 °C. Yield 0.61 g (73%). Elemental analysis, found (calcd): C 65.7 (65.6); H 8.0 (8.4). ^{1}H NMR (C_6D_6): 7.30 (s, 1H), 2.87 (m, 1H), 2.45 (m, 1H), 2.33 (m, 1H), 1.76

(29) Chamberlain, B. M.; Sun, Y.; Hagadorn, J. R.; Hemmesch, E. W.; Young, V. G., Jr.; Pink, M.; Tolman, W. B. *Macromolecules* **1999**, *32*, 2400−2402.

(30) Trofimenko, S.; Calabrese, J. C.; Thompson, J. S. *Inorg. Chem.* **1987**, *26*, 1507.

(31) Dias, H. V. R.; Gordon, J. D. *Inorg. Chem.* **1996**, *35*, 318.

Table 7. Summary of Crystallographic Data[a]

	1	2	3	4
empirical formula	$C_{33}H_{35}BMgN_6O$	$C_{34}H_{55}BN_6Zn$	$C_{20}H_{23}BF_{12}N_6OSiZn$	$C_6H_8O_4$
color	colorless	colorless	colorless	colorless
crystal dimensions (mm)	.35 × 0.35 × 0.30	.075 × 0.25 × 0.50	.32 × 0.30 × 0.30	.25 × .30 × 0.30
space group	$P2_1/n$	$P2_12_12_1$	*Pbca*	$P2_1/C$
cell dimensions				
temp (°C)	−122	−168	−163	−172
a (Å)	14.657(1)	17.790(3)	31.194(1)	7.730(4)
b (Å)	14.339(1)	19.951(4)	10.858(1)	9.836(6)
c (Å)	15.315(1)	9.712(2)	34.225(1)	9.402(1)
α (deg)				
β (deg)	104.20(0)			110.03(4)
γ (deg)				
Z	4	4	16	4
V	3120.40	3446.85	11592.06	671.67
D_{calc} (g cm^{-3})	1.207	1.203	1.595	1.425
wavelength	.71069	.71069	.71073	.71069
molecular weight	566.79	624.05	695.71	144.13
linear abs coeff cm^{-1}	.873	7.442	9.926	1.137
detector to sample distance (cm)	22.5	22.5	5.0	22.5
sample to source distance (cm)	23.5	23.5	2./5	
take off angle (deg)	2.0	2.0	6.0	2.0
scan speed (deg/min)	8.0	6.0	*b*	6.0
scan width (deg)	2.0	2.0	*b*	2.0
aperture size	3.0 × 4.0		*b*	3.0 × 4.0
2*θ* range, (deg)	6−50	6−50	0−60	6−50
total reflections collected	9187	8051	116954	1286
no. unique intensities	5487	6086	16992	1181
no. with $F > 0.0$	4828	5874	15749	1074
no. with $F > 2.33\sigma(F)$	3501		8195	886
no. with $F > 3\sigma(F)$		5121		
$R(F)$[c]	.0591	.0549	0.0322	0.974
$R_w(F)$[c]	.0465	.0520	0.0252	0.890
goodness of fit	1.489	1.125	0.671	3.203
maximum Δ/σ	0.05	0.016	0.02	0.32

[a] **1** = HB(3-Phpz)$_3$Mg−CH_2CH_3.THF; **2** = HB($C_{11}H_{17}N_2$)$_3$Zn−CH_3; **3** = HB(3,5-$(CF_3)_2$pz)$_2$(3-^{t}Bupz)Zn−O−Si$(CH_3)_3$; **4** = *meso*-lactide [b] Data collected on the Bruker Smart 6000 system using frame width of 0.3° and time per frame 60.1 s [c] $R(F) = \Sigma||F_o| - |F_c||/\Sigma|F_o|$; $R_w(F) = \{\Sigma w(|F_o| - |F_c|)^2/\Sigma w|F_o|^2\}^{1/2}$, where $w = 1/[|\sigma^2||F_o|]$.

(m, 1H), 1.51 (m, 1H), 1.26 (m, 1H), 1.09 (d, 3H, $J = 5.1$ Hz), 0.77 (d, 3H, $J = 4.8$ Hz), 0.29 (s, $ZnCH_3$).

[η^3-HB(3^{t}Bupz)$_3$]MgOEt, 3. [η^3-HB(3^{t}Bupz)$_3$]Tl, (1.0 g, 17.1 mmol) was dissolved in THF (10 mL) cooled at 0 °C. To this solution was added Et_2Mg (17.1 mL of a 1 M solution in Et_2O). There was an immediate formation of Tl metal. The mixture was stirred for 30 min at 0 °C, warmed to room temperature, and stirred with a magnetic spin bar for a further 30 min. The solution was filtered through Celite, and the solvent was removed. The ^{1}H NMR of the resultant white solid was recorded and was found to agree with that reported for [η^3-HB(3-^{t}Bupz)$_3$]MgEt by Parkin. This compound (0.5 g, 1.1 mmol) was then dissolved in benzene (10 mL) and 1 equiv of EtOH (1.1 mL of a 1 M solution of EtOH in benzene) was added dropwise with stirring in a cold water bath. The reaction mixture was stirred for 30 min and allowed to warm to room temperature. The solvent was removed in vacuo to yield a fluffy white solid: [η^3-HB(3-^{t}Bupz)$_3$]Mg(OEt) (0.3 g, 57% yield) ^{1}H NMR (C_6D_6) 7.30 (d, 1H, $J = 1.5$ Hz), 6.10 (d, 1H, $J = 1.5$ Hz), 4.60 (q, 2H, $J = 6.8$ Hz), 1.48 (s, 9H), 1.72 (t, 3H, $J = 6.8$ Hz). This compound is extremely soluble in hydrocarbon solvents, and all attempts to obtain crystals suitable for single-crystal X-ray diffraction failed.

[η^3-HB((7*R*)-^{i}Pr-(4*R*)-Me-4,5,6,7-tetrahydro-2H-indazolyl)$_3$]Mg-(OPh), 4. Compound **4** was made in a manner directly analogous to compound **3** wherein PhOH (purified by sublimation) in benzene was used in place of EtOH. Compound **4** is a white solid, air-sensitive and soluble in all common hydrocarbon solvents. ^{1}H NMR (C_6D_6): 7.45 (t, 2H, $J = 5.1$ Hz), 7.30 (s, 3H), 7.19 (d, 2H, $J = 4.0$ Hz), 6.90 (t, 1H, $J = 4.0$ Hz), 2.86 (m, 3H), 2.44 (m, 3H), 1.69 (m, 3H), 1.46 (m, 6H), 1.24 (m, 6H), 1.05 (d, 9H, $J = 3.9$ Hz), 0.98 (d, 9H, $J = 4.2$ Hz), 0.77 (d, 3H, $J = 4.2$ Hz).

[η^3-HB(3-Phpz)$_3$]MgEt(THF). A reaction was carried out between $MgEt_2$ and [η^3-HB(3-Phpz)$_3$]Tl as described for **3** above. Crystals suitable for an X-ray study were obtained by slowly cooling at THF soln to −10 °C. ^{1}H NMR (C_6D_6): 7.59 (d, 6H, $J = 5.4$ Hz), 7.47 (d, 3H, $J = 1.5$ Hz), 7.15 (t, 6H, J − 4.5 Hz), 6.10 (d, 3H, $J = 1.5$ Hz), 1.09 (t, 3H, $MgCH_2CH_3$), $J = 6.8$ Hz), 1.10 (q, $MgCH_2CH_3$, $J = 6.8$ Hz).

[η^3-HB(3-^{t}Bupz)(3,5-$(CF_3)_2$pz)$_2$]K. 3-^{t}Bupz (0.50 g, 4.03 mmol) was added to a solution of KH_2B (3,5-$(CF_3)_2$pz)$_2$ (1.84 g, 4.03 mmol) in toluene (10 mL). The mixture was stirred with a magnetic spin bar and refluxed under an atmosphere of dry nitrogen for 5 days. The solvent was then removed under a dynamic vacuum, and the resultant solids were washed with petroleum ether (boiling range 35−60 °C). The white solids were collected by filtration and then extracted into CH_2Cl_2. The soluble extracts were collected, and the volume of the solution was reduced under a dynamic vacuum. Crystallization from CH_2Cl_2 gave the potassium salt as a white microcrystalline powder (1.9 g, 81% yield). ^{1}H NMR (C_6D_6): 7.71 (d, 1H), 6.32 (s, 2H), 5.90 (d, 1H), 0.99 (s, 9H). ^{19}F NMR (C_6D_6) −59.05 (d, 6F), −61.84 (s, 6F).

[η^3-HB(3-^{t}Bupz)(3,5-$(CF_3)_2$pz)$_2$]Tl. A solution of the potassium salt above (0.50 g, 0.862 mmol) in CH_2Cl_2 (10 mL) was added to TlOAc (0.275 g, 1.03 mmol) in CH_2Cl_2 (20 mL). The solution was stirred overnight, during which a white precipitate formed. The solution was collected by filtration, and the solvent was reduced under a dynamic vacuum to yield the thallium salt as white microcrystalline solid (0.36 g, 56% yield). ^{1}H NMR (C_6D_6): 7.56 (d, 1H), 6.24 (s, 2H), 5.86 (d, 1H), 1.07 (s, 9H). ^{19}F NMR (C_6D_6): −59.15 (d, 6F), −59.50 (br, 3F), −61.54 (br, 3F).

[η^3-HB(3-^{t}Bupz)(3,5-$(CF_3)_2$pz)$_2$]ZnCl. A solution of $ZnCl_2$ (0.065 g, 0.48 mmol) in THF (5 mL) was added to a solution of the thallium salt prepared above (0.30 0 g, 0.402 mmol) in THF (10 mL). A white precipitate formed immediately. The solution was stirred for 1 h and then filtered. The soluble portion was collected, and the solvent was removed under a dynamic vacuum. The product was extracted with

benzene and recrystallized from CH_2Cl_2 to give a fine white powder (0.20 g, 76% yield). ^{1}H NMR (C_6D_6): 7.00 (d, 1H), 5.94 (s, 2H), 5.64 (d, 1H), 1.32 (s, 9H). ^{19}F NMR (C_6D_6): −59.62 (d, 6F), −60.52 (s, 6F).

[η^3-HB(3-^{t}Bupz)(3,5-(CF$_3$)$_2$pz)$_2$]ZnOSiMe$_3$, 5. A solution of [η^3-HB(3-^{t}Bupz)(3,5-(CF$_3$)$_2$pz)$_2$]ZnCl (0.300 g, 0.467 mmol) in CH_2Cl_2 (50 mL) was cooled to 0 °C. To this solution was added $NaOSiMe_3$ (0.500 mL of a 1 M solution in CH_2Cl_2, 0.500 mmol) dropwise with stirring. The resultant solution was stirred for 20 min and allowed to warm to room temperature. The mixture was filtered to remove NaCl, and the CH_2Cl_2 extract was collected. Crystallization from CH_2Cl_2 yielded colorless crystals of compound **5** (0.24 g, 75% yield). In the solid-state compound **5** is stable (inert) to air at room temperature for several hours. [It is important to use $NaOSiMe_3$ in the preparation given above as the $KOSiMe_3$ yields a mixture of products because some [η^3-HB(3-^{t}Bupz)(3,5-(CF$_3$)$_2$pz)$_2$]K is formed by metathesis. ^{1}H NMR (C_6D_6): 7.01 (d, 1H), 5.95 (s, 2H), 5.63 (d, 1H), 1.32 (s, 9H), 0.61 (s, 9H, $SiMe_3$)**.** ^{19}F NMR (C_6D_6): −59.74 (d, 6F), −61.13 (s, 6F).

NOE Difference Spectra. The spectra were recorded for solutions of **1** and **3** in CD_2Cl_2 in the presence of 100 equiv of propylene oxide. Irradiation of the PO methyl signal led to a 4 and 5% signal difference in the ^{t}Bu signals of the zinc and magnesium compounds, respectively. Similarly, while [η^3-HB(3-^{t}Bupz)$_3$]MgEt showed no ability to polymerize L-lactide in CH_2Cl_2, irradiation of the lactide methyl signal gave a 3% NOE difference for the ^{t}Bu signal in the ^{1}H NMR NOE difference spectrum.

NMR Tube Polymerizations. In this work kinetic data were obtained from ^{1}H NMR studies of polymerizations carried out in CD_2Cl_2 solutions for the zinc complexes. For magnesium catalysts benchtop polymerizations were carried out in CH_2Cl_2 wherein aliquots were removed from the reaction mixture and the lactide to PLA ratio was then determined in C_6D_6 by ^{1}H NMR, having first removed the CH_2Cl_2 under a dynamic vacuum. The reactions were followed by integrating the lactide methyl signal and the methyl protons of the polymer as a function of time. A representative procedure is given below. Compound **1** (20 mg, 0.037 mmol) and L-lactide (537 mg, 3.7 mmol) were placed in two separate vials in the drybox and were dissolved in 0.2 mL and 0.3 mL of CD_2Cl_2, respectively. The contents of the two vials were then removed, and the reaction mixture was placed into a J. Young NMR tube (to prevent solvent evaporation). The reaction was followed by ^{1}H NMR spectroscopy at 22 °C until polymerization was 90% complete. The delay time was chosen to be 10 s and 16 scans as the number of transients.

Plots of ln([lactide]$_{t=t'}$/[lactide]$_{t=0}$) versus time gave straight lines. The rates of polymerization increased with increasing concentration of catalyst: doubling the concentration of catalyst doubled the rate, consistent with a first-order dependence on metal catalyst. Further data are given in the Supporting Information.

Cystallographic Studies. Crystallographic procedures have been given previously.[32] A summary of crystal data for the four compounds studied in this work is given in Table 7.

Molecular Weight Determination. For [η^3-HB(3^{t}Bupz)$_3$]MgOEt a Signer molecular weight determination was used.[33] The Signer method involves allowing a solution of the analyte and a solution of a standard to come to molar concentration equilibrium by allowing solvent vapors to move from the dilute solution to the concentrated one. Anthracene was used as a standard for the experiment performed in this study.

Acknowledgment. This paper is dedicated to Professor D. C. Bradley on the occasion of his 75th birthday. We thank the Department of Energy, Office of Basic Energy Sciences, Chemistry Division for support. N. W. E. acknowledges the National Science and Engineering Research council of Canada for a postdoctoral fellowship. K. P. acknowledges the Institute for the Promotion of Teaching Science and Technology (IPST), Thailand, for an opportunity to work on this project. We also thank the reviewers and Prof. G. Parkin for helpful comments.

Supporting Information Available: Representative kinetic plots; MW vs % converstion plots of **1** and **3**; NMR stacked plots of the polymerization of 1:1 *rac*:*meso* lactide using **1** and **2**; plot of measured vs theoretical molecular weight of poly(L-lactide) using **3**; and crystallographic data for: HB(3-^{t}Bupz)$_3$ZnOSiMe$_3$·toluene; HB(3-Phpz)$_3$Mg−CH$_2$CH$_3$·(THF); HB(C$_{11}$H$_{17}$N$_2$)$_3$Zn−CH$_3$; HB(3,5-(CF$_3$)$_2$pz)$_2$(3-^{t}Bupz)-ZnOSiMe$_3$ and *meso*-lactide (PDF). This material is available free of charge via the Internet at http://pubs.acs.org.

JA002160G

(32) Chisholm, M. H.; Folting, K.; Huffman, J. C.; Kirkpatrick, C. C. *Inorg. Chem.* **1984**, *23*, 1021−1022.
(33) Clark, E. P. *Ind. Eng. Chem., Anal. Ed.* **1941**, *13*, 820.